Soft Supersymmetry Breaking and Radiative Higgs Signatures

HONG-JIAN HE
*University of Texas at Austin**

I review our recent formulation of the *minimal* FCNC schemes of the soft supersymmetry breaking via the squark mass-terms and scalar trilinear interactions, where the large $O(1)$ mixings among scalar-tops and -charms are found to be consistent with all existing theoretical and experimental bounds. Such a feature is demonstrated in a class of attractive new models with horizontal $U(1)$ symmetry which also explain the observed quark-mass pattern and solve the SUSY μ-problem. The soft SUSY breaking induced radiative $H^{\pm}bc$ and h^0tc Higgs couplings are analyzed and are shown to provide exciting new discovery Higgs signatures at the Tevatron and LHC.

1. Introduction

Understanding the flavor structure poses a major challenge to the weak-scale supersymmetry (SUSY) [1], which necessarily extends the standard model (SM) flavor sector with three-family superpartners for all fermions and thus *adds* further puzzles to the flavor physics. The supersymmetry must be also softly broken, to account for the mass gaps between the SM particles and non-observed superpartners while remaining to stabilize the weak scale against radiative corrections. This is parametrized by the soft-breaking Lagrangian of Minimal Supersymmetric SM (MSSM) in which the flavor sector contains a large number of free parameters and is often problematic with low-energy flavor changing neutral current (FCNC) constraints without additional simplifying assumptions. The usual assumption about the proportionality of scalar trilinear A-terms to fermion Yukawa couplings, for instance, is not generic from string-theory constructions and some interesting implications of non-diagonal A-terms have been recently studied [2, 3]. Indeed, exploring the SUSY flavor sector is important for unravelling the mechanism of soft SUSY breaking as well as for discovering new signatures from the weak-scale supersymmetry.

Our recent attempt [4] focuses on the flavor-mixings of three-family squarks which enter the soft-breaking Lagrangian via scalar mass-terms and trilinear interactions. We first formulate a viable *minimal* SUSY FCNC scenario, called Type-A, in which all visible FCNC effects are solely from the non-diagonal trilinear A-term in the scalar top-charm ($\tilde{t}-\tilde{c}$) sector, consistent with all existing constraints. Then, based upon the simplest horizontal $U(1)$ symmetry, we construct a class of attractive new models, called Type-B, which exhibit similar but richer flavor-mixings in the $\tilde{t}-\tilde{c}$ sector. This construction also nicely explain the observed quark-mass/mixing pattern and solve the SUSY μ-problem. As applications, we then analyze supersymmetric radiative corrections to the $H^{\pm}bc$ and h^0tc vertices, and study new discovery collider signatures of charged Higgs via charm-bottom fusion [7] and the flavor changing top-decays into the charm and lightest neutral Higgs.

2. Minimal SUSY FCNC Models

We start by observing that the current data have mainly suppressed the FCNCs associated with the first two family squarks and in some cases with the first and third families, but still allow flavor-mixings of the second- and third-family scharm ($\tilde{c}$) and stop ($\tilde{t}$) to be naturally as large as $O(1)$ [5]. Furthermore, the $O(1)$ $\tilde{t}-\tilde{c}$ mixings arising from the non-diagonal A-term are consistent with all theoretical bounds by charge-color breaking (CCB) and vacuum stability (VS) [6]. Using this bottom-up approach, a viable *minimal* SUSY FCNC scenario (called Type-A) is formulated with a minimal non-diagonal trilinear A-term. Then, based on the simplest horizontal $U(1)$ symmetry,

*hjhe@physics.utexas.edu

a class of new models (called Type-B) are constructed, which exhibit similar flavor-mixings in the $\tilde{t}-\tilde{c}$ sector, as well as explain the observed quark-mass/mixing pattern and the natural size of SUSY μ-parameter. Besides economics, such minimal FCNC schemes allow us to reduce the general 6×6 squark-mass-matrics down to typical 4×4 or 3×3 matrices involving only the $\tilde{c}-\tilde{t}$ sector, making the exact squark mass-diagonalization and rotations feasible, without relying on the popular but crude mass-insertion approach. This allows quantitative understanding of the relevant FCNC signatures from the squark sector, and thus reliably probes the fundamental SUSY flavor structure of the soft-breaking Lagrangian.

2.1. Type-A Models

The MSSM soft-breaking squark-sector contains following quadratic mass-terms and trilinear A-terms,

$$
\begin{aligned}
&-\widetilde{Q}_i^\dagger (M^2_{\widetilde{Q}})_{ij}\widetilde{Q}_j - \widetilde{U}_i^\dagger (M^2_{\widetilde{U}})_{ij}\widetilde{U}_j - \widetilde{D}_i^\dagger (M^2_{\widetilde{D}})_{ij}\widetilde{D}_j \\
&+(A_u^{ij}\widetilde{Q}_i H_u \widetilde{U}_j - A_d^{ij}\widetilde{Q}_i H_d \widetilde{D}_j + \text{c.c.})\,,
\end{aligned}
\tag{1}
$$

with $M^2_{\widetilde{Q},\widetilde{U},\widetilde{D}}$ and $A_{u,d}$ being 3×3 matrices in squark flavor-space. This gives a generic 6×6 mass matrix,

$$
\widetilde{\mathcal{M}}_u^2 = \begin{bmatrix} M^2_{LL} & M^2_{LR} \\ M^{2\,\dagger}_{LR} & M^2_{RR} \end{bmatrix},
\tag{2}
$$

in the up-squark sector, where

$$
\begin{aligned}
M^2_{LL} &= M^2_{\widetilde{Q}} + M^2_u + \tfrac{1}{6}\cos 2\beta\,(4m^2_w - m^2_z)\,, \\
M^2_{RR} &= M^2_{\widetilde{U}} + M^2_u + \tfrac{2}{3}\cos 2\beta \sin^2\theta_w\, m^2_z\,, \\
M^2_{LR} &= A_u v \sin\beta/\sqrt{2} - M_u\,\mu\cot\beta\,,
\end{aligned}
\tag{3}
$$

with M_u the up-quark mass matrix and $m_{w,z}$ the masses of $(W^\pm,\, Z^0)$. For convenience, we choose the super Cabibbo-Kobayashi-Maskawa (CKM) basis for squarks so that in Eq. (3), $A_u \to A'_u = K_{UL}A_u K^\dagger_{UR}$ and $M_u \to M_u^{\text{diag}}$, etc, with $K_{UL,R}$ the rotation matrices for M_u diagonalization. In our *minimal* Type-A scheme, we consider all large FCNCs to *solely* come from non-diagonal A'_u in the up-sector, and those in the down-sector to be negligible. Thus, we define, at the weak scale,

$$
A'_u = \begin{bmatrix} 0 & 0 & 0 \\ 0 & 0 & x \\ 0 & y & 1 \end{bmatrix} A\,,
\tag{4}
$$

where, $(x,\, y) = O(1)$, represent naturally large flavor-mixings associated with $\tilde{t}-\tilde{c}$ sector. Such a minimal scheme of SUSY FCNC is compelling as it is fully consistent with the strigent CCB/VS theory bounds [6] and the existing data [5]. (In the case that the CKM matrix is generated from down-quark sector only [3], A'_u simply reduces back to A_u.) Similar pattern may be also defined for A_d in the down-sector, but the strong CCB/VS bounds permits $O(1)$ $\tilde{b}-\tilde{s}$ mixings only for very large $\tan\beta$ because $m_b \ll m_t$. To allow full range of $\tan\beta$, we consider an almost diagonal A_d. Defining non-diagonal A_u as the only visible FCNC source in Type-A schemes also requires nearly diagonal squark-mass-matrices $M^2_{\widetilde{Q},\widetilde{U}}$ in Eqs. (2)-(3), and we can define, for simplicity, $M^2_{LL} \simeq M^2_{RR} \simeq \widetilde{m}_0^2\,\mathbf{I}_{3\times 3}$, with $\widetilde{m}_0$ a common scale of scalar-masses [8].

From this minimal Type-A scheme, we find that the first family squarks $\tilde{u}_{L,R}$ decouple from the rest in (2) so that the 6×6 mass-matrix is reduced to 4×4,

$$
\widetilde{\mathcal{M}}_{ct}^2 = \begin{bmatrix} \widetilde{m}_0^2 & 0 & 0 & A_x \\ 0 & \widetilde{m}_0^2 & A_y & 0 \\ 0 & A_y & \widetilde{m}_0^2 & X_t \\ A_x & 0 & X_t & \widetilde{m}_0^2 \end{bmatrix}
\tag{5}
$$

for squarks $(\tilde{c}_L, \tilde{c}_R, \tilde{t}_L, \tilde{t}_R)$, where

$$\begin{aligned} &A_x = x\widehat{A}, \quad A_y = y\widehat{A}, \quad \widehat{A} = Av\sin\beta/\sqrt{2}\,, \\ &X_t = \widehat{A} - \mu\, m_t \cot\beta\,. \end{aligned} \tag{6}$$

Tiny terms of $O(m_c)$ or smaller are ignored in Eq. (5). The reduced squark mass matrix (5) has 6 zero-entries in total and is simple enough for an elegant exact diagonalization. Especially, for two typical cases of (i) $x \neq 0,\ y = 0$, (called Type-A1) and (ii) $x = 0,\ y \neq 0$, (called Type-A2), we have one more squark $\tilde{c}_R$ (in Type-A1) or $\tilde{c}_L$ (in Type-A2) decouple from the rest so that Eq. (5) further reduces to a 3×3 matrix, allowing a much simpler exact diagonalization. We have worked out the general analytic diagonalization of 4×4 matrix (5) for any (x, y). The mass-eigenvalues of the eigenstates $(\tilde{c}_1, \tilde{c}_2, \tilde{t}_1, \tilde{t}_2)$ are,

$$\begin{aligned} M^2_{\tilde{c}1,2} &= \widetilde{m}_0^2 \mp \tfrac{1}{2}\left|\sqrt{\omega_+} - \sqrt{\omega_-}\right|, \\ M^2_{\tilde{t}1,2} &= \widetilde{m}_0^2 \mp \tfrac{1}{2}\left|\sqrt{\omega_+} + \sqrt{\omega_-}\right|, \end{aligned} \tag{7}$$

where $\omega_\pm = X_t^2 + (A_x \pm A_y)^2$. From (7), we can deduce the mass-spectrum of stop-scharm sector,

$$M_{\tilde{t}1} < M_{\tilde{c}1} < M_{\tilde{c}2} < M_{\tilde{t}2}\,. \tag{8}$$

The stop $\tilde{t}_1$ can be as light as 120 − 300 GeV for the typical range of $\widetilde{m}_0 \gtrsim 0.5 - 1$ TeV. We then deduce the 4×4 rotation matrix of the diagonalization,

$$\begin{aligned} &\begin{pmatrix} \tilde{c}_L \\ \tilde{c}_R \\ \tilde{t}_L \\ \tilde{t}_R \end{pmatrix} = \begin{pmatrix} c_1c_3 & c_1s_3 & s_1s_4 & s_1c_4 \\ -c_2s_3 & c_2c_3 & s_2c_4 & -s_2s_4 \\ -s_1c_3 & -s_1s_3 & c_1s_4 & c_1c_4 \\ s_2s_3 & -s_2c_3 & c_2c_4 & -c_2s_4 \end{pmatrix} \begin{pmatrix} \tilde{c}_1 \\ \tilde{c}_2 \\ \tilde{t}_1 \\ \tilde{t}_2 \end{pmatrix}, \\ &s_{1,2} = \frac{1}{\sqrt{2}}\left[1 - \frac{X_t^2 \mp A_x^2 \pm A_y^2}{\sqrt{\omega_+\omega_-}}\right]^{1/2}, \quad s_4 = \frac{1}{\sqrt{2}}\,, \end{aligned} \tag{9}$$

and $s_3 = 0$ (if $xy = 0$), or, $s_3 = 1/\sqrt{2}$ (if $xy \neq 0$), where $s_j^2 + c_j^2 = 1$. With the rotation (9) we can derive all relevant new Feynamn rules in mass-eigenstates without relying on the crude mass-insertion method.

2.2. Type-B Models with Horizontal $U(1)$ Symmetry

The minimal Type-A SUSY FCNC schemes with non-diagonal A_u-term are truely economic as they unqiuely result from imposing all the stringent theoretical and experimental bounds. We will further support such FCNC in the $\tilde{t} - \tilde{c}$ sector by providing theoretically compelling constructions based upon a minimal family symmetry. An attractive approach is to make use of the simplest horizontal $U(1)$ symmetry for generating realistic flavor structure of both quarks and squarks (via proper powers of a single suppression factor [9, 10]), which also solves the SUSY μ-problem altogether. We define this suppression factor $\varepsilon = \langle S\rangle/\Lambda$ to have similar size to the Wolfenstein-parameter λ of CKM, i.e., $\varepsilon \simeq \lambda \simeq 0.22$ [10], where $\langle S\rangle$ is vacuum expectation value of a singlet scalar S for spontaneous $U(1)$ breaking and Λ is the scale at which the $U(1)$ breaking is mediated to light fermions. The supermultiplets of three-family quarks/squarks are differently charged under $U(1)$, as shown in Table I.

Table I Quantum number assignments under the horizontal symmetry $U(1)_H$.

Q_1	Q_2	Q_3	$\overline{u}_1$	$\overline{u}_2$	$\overline{u}_3$	$\overline{d}_1$	$\overline{d}_2$	$\overline{d}_3$	H_u	H_d	S
h_1	h_2	h_3	α_1	α_2	α_3	β_1	β_2	β_3	ξ	ξ'	-1

Then, the following hierarchy structures can be deduced in the quark mass matrices,

$$M_u^{ij} \sim \frac{v_u}{\sqrt{2}}\lambda^{\alpha_i+h_j+\xi}\,, \quad M_d^{ij} \sim \frac{v_u}{\sqrt{2}}\frac{1}{\tan\beta}\lambda^{\beta_i+h_j+\xi'}\,, \tag{10}$$

and in the CKM matrix,

$$(V_{us}, V_{cb}, V_{ub}) \sim \left(\lambda^{h_1-h_2}, \lambda^{h_2-h_3}, \lambda^{h_1-h_3}\right)\,. \tag{11}$$

Different from Ref. [10], the key ingredient of our model-buildings is to impose a new condition,

$$\alpha_2 = \alpha_3 \tag{12}$$

which ensures natural $O(1)$ mixings between $\tilde{c}$ and $\tilde{t}$ in the squark mass matrix. From the condition (12) and the current data of quark-masses and CKM angles (which can all be counted in powers of λ), and after a lengthy systematic analysis, we find an almost unique solution for all quark/squark quantum numbers (cf., Table **??**). We will call this the *minimal* Type-B scheme hereafter. In Table **??**, we consider $\tan\beta \sim O(1)$ for the down-sector. The extension to larger $\tan\beta$ only affects quantum numbers of $\overline{d}_j$'s in a trivial manner as it only contributes an overall factor $1/\tan\beta \sim \lambda^k$ (with integer $k \sim 0.66\log\tan\beta$) to M_d in Eq. (10) and thus simply adds $-k$ to each quantum number of $\overline{d}_j$ in Table II.

Table II Quantum number assignments are derived for minimal Type-B model.

Q_1	Q_2	Q_3	$\overline{u}_1$	$\overline{u}_2$	$\overline{u}_3$	$\overline{d}_1$	$\overline{d}_2$	$\overline{d}_3$	H_u	H_d	S
4	3	0	$3-\xi$	$-\xi$	$-\xi$	$4-\xi'$	$3-\xi'$	$3-\xi'$	ξ	ξ'	-1

Some variations of this minimal Type-B model can be constructed, depending on if the quantum numbers of Q_j's are allowed to contain $\xi(\xi')$, but they all share same predictions for masses and mixings. Here, we have attempted to simultaneously solve the SUSY μ-problem from the same $U(1)$. We thus have a dynamical μ-term from $(\kappa/\Lambda^{n-1})S^n H_u H_d$ $(n = \xi + \xi')$ such that $\mu = \kappa\lambda^{n-1}\langle S\rangle$ is generated at a scale $\langle S\rangle \ll M_{\rm Planck}$. A weak-scale value of μ is obtained by properly choosing n for a given $\langle S\rangle$. If this $U(1)$ is not responsible for a μ-solution, the minimal Type-B model becomes truely unique, corresponding to the special case of $\xi = \xi' = 0$ in Table II. From Table II, the structures of quark/squark-mass-matrices can be readily deduced. For instance, the up-quark mass-matrix takes the form,

$$M_u \sim \frac{v_u}{\sqrt{2}}\begin{bmatrix} \lambda^7 & \lambda^4 & \lambda^4 \\ \lambda^6 & \lambda^3 & \lambda^3 \\ \lambda^3 & 1 & 1 \end{bmatrix}, \tag{13}$$

for any $\tan\beta \gtrsim 1$, while the squark mass-matrices M_{LL}^2 and M_{RR}^2 in Eq. (2) are derived as,

$$\begin{aligned} M_{LL}^2 &\sim \widetilde{m}_0^2\begin{bmatrix} 1 & \lambda & \lambda^4 \\ \lambda & 1 & \lambda^3 \\ \lambda^4 & \lambda^3 & 1 \end{bmatrix}, \\ M_{RR}^2 &\sim \widetilde{m}_0^2\begin{bmatrix} 1 & \lambda^3 & \lambda^3 \\ \lambda^3 & 1 & 1 \\ \lambda^3 & 1 & 1 \end{bmatrix}. \end{aligned} \tag{14}$$

Eqs. (13) and (14) show a partial quark-squark "alignment" that effectively suppresses the FCNCs between 1st and 2nd(3rd) families, while at the same time provides $O(1)$ mixings in $\tilde{t}-\tilde{c}$ sector of M_{RR}^2. Further $\tilde{t}-\tilde{c}$ mixings come from non-diagonal A_u which is now *predicted* to share the same hierarchy structure in Eq. (13) as M_u since squark carries same $U(1)_H$-charge as quark. This, however, does not imply exact "proportionality" between A_u and M_u because the power-counting of λ allows an $O(1)$ coefficient undetermined which can generally invalidate $A_u \propto M_u$. Ignoring small $O(\lambda^3) \simeq 1\%$ terms, we can diagonalize M_u by a 2×2 rotation of singlet quarks $(\bar{c},\, \bar{t})$. Then, the off-diagonal block M^2_{LR} in Eq. (2) takes the form, under the super-CKM basis,

$$M^2_{LR} \;=\; A'_u v \sin\beta/\sqrt{2} - M_u^{\rm diag}\,\mu\cot\beta\,, \tag{15}$$

with $A'_u \;=\; K_{UL}A_u K^\dagger_{UR} \;=\; A_u K^\dagger_{UR} + O(\lambda^3)$ in which the singlet-quark rotation K_{UR} only contains a nontrivial sub-matrix involving (2nd, 3rd)-families. Upon neglecting tiny $O(\lambda^3)$ terms, we parametrize the *minimal* A'_u of Type-B by introducing a parameter $y = O(1)$,

$$A'_u = \begin{bmatrix} 0 & 0 & 0 \\ 0 & 0 & 0 \\ 0 & y & 1 \end{bmatrix} A\,. \tag{16}$$

Then, the squarks $(\tilde{u}_L,\, \tilde{u}_R,\, \tilde{c}_L)$ are found to decouple from the rest so that Eq. (2) greatly reduces to a 3×3 matrix, which takes the form, in the basis $(\tilde{c}_R,\, \tilde{t}_L,\, \tilde{t}_R)$,

$$\widetilde{M}^2_{ct}[\mathrm{B}] = \begin{bmatrix} \widetilde{m}^2_0 & A_y & x\widetilde{m}^2_0 \\ A_y & \widetilde{m}^2_0 & X_t \\ x\widetilde{m}^2_0 & X_t & \widetilde{m}^2_0 \end{bmatrix}, \tag{17}$$

where $A_y = yAv\sin\beta/\sqrt{2}$ and $x = O(1)$ characterizes $\tilde{c}_R - \tilde{t}_R$ mixings in M^2_{RR} [cf., Eq. (14)]. The Type-B contains two typical schemes called Type-B1 ($y = 0$) and Type-B2 ($x = 0$). We observe that Scheme-B2 is just *identical* to our Scheme-A2, as they share the same form of non-diagonal A_u. Also, Type-B1 matrix with $y = 0$ in Eq. (17) takes the same structure as that of Type-A1 except that Eq. (17) involves $\tilde{c}_R$ (not $\tilde{c}_L$) and its x originates from M^2_{RR} (not A_u). More elaborated analyses are given in [4], but the following summary of collider studies in typical Scheme-A1, -A2 and -B2 represents the main features of both Type-A and Type-B signals.

3. SUSY Radiative Corrections to $H^\pm bc$ and $h^0 tc$ Vertices

The soft SUSY-breaking induced radiative FCNC couplings conceptually differ from that in Ref. [7] because the MSSM Higgs sector has no tree-level FCNC. With the exact diagonalization of Eq. (9), we first calculate the dominant SUSY-QCD radiative corrections to the $H^\pm bc$ vertex. These are vertex corrections [scharm(stop)-sbottom-gluino loop] and self-energy corrections [scharm(stop)-gluino loop], which we define as,

$$\begin{aligned} \Gamma_{H^+ b\bar{c}} \;&=\; i\,\overline{u}_c(k_2)\,(F_L P_L + F_R P_R)\,u_b(k_1)\,, \\ F_{L,R} \;&=\; F^0_{L,R} + F^V_{L,R} + F^S_{L,R}\,, \end{aligned} \tag{18}$$

where $P_{L,R} = (1 \mp \gamma_5)/2$ and the tree-level results are,

$$(F^0_L,\, F^0_R) = \frac{gV_{cb}}{\sqrt{2}m_w}\,(m_c\cot\beta,\; m_b\tan\beta)\,, \tag{19}$$

with V_{cb} from the CKM matrix. The one-loop vertex corrections in Type-A1 are,

$$\begin{aligned} F^V_L \;&=\; 0\,, \\ F^V_R \;&=\; \frac{\alpha_s}{3\pi} m_{\tilde{g}} \sum_{j,k} \kappa^R_{jk} C_0(m^2_H, 0, 0; m_{\tilde{b}_j}, m_{\tilde{g}}, m_{\tilde{u}_k}), \end{aligned} \tag{20}$$

where $\tilde{u}_k \in (\tilde{c}_2, \tilde{t}_1, \tilde{t}_2)$, $\tilde{b}_j \in (\tilde{b}_1, \tilde{b}_2)$, and C_0 is the 3-point C-function of Passarino-Veltman (PV). κ^R_{jk} is the product of relevant $H^\pm - \tilde{b}_j - \tilde{u}_k$, $\tilde{b}_j - \tilde{g} - b$ and $\tilde{u}_k - \tilde{g} - c$ couplings, derived with rotation (9) and we also include the $\tilde{b}_L - \tilde{b}_R$ mixing, which may be sizable for large $\tan\beta$. The Type-A1 self-energy corrections are, $F^S_L = 0$, and

$$F^S_R = \hat{F}^0_R \frac{\alpha_s s_1}{3\pi} \frac{m_{\tilde{g}}}{m_t} \sum_{j=1,2} (-)^{j+1} B_0(0; m_{\tilde{g}}, m_{\tilde{t}_j}), \tag{21}$$

with B_0 the 2-point PV function and s_1 given in Eq.(9) for $y = 0$. $(\hat{F}_L^0, \hat{F}_R^0) = (gV_{tb}/\sqrt{2}m_w)(m_t\cot\beta,\, m_b\tan\beta)$ are tree-level $H^\pm tb$ couplings. In Eqs.(20)-(21), the tiny sub-leading terms suppressed by powers of $m_c/m_{t,\tilde{g}}$ are ignored. The $F_{L,R}^{V,S}$ in Type-A2 and Type-B2 can be obtained from Eqs.(20)-(21) via exchanges of $L \leftrightarrow R$ and $x \to y$. Note that $F_{L(R)}$ vanishes in Type-A1(-A2,B2) due to its specific chirality structure.

Next, we turn to analyze the flavor-changing top-decay $t \to ch^0$ in our schemes. This decay is always kinematically allowed in the MSSM. Since the SM branching ratio of this decay is at the level of $10^{-13} - 10^{-14}$ or smaller [13], this channel thus becomes an excellent window for detecting new physics [14]. The radiative tch^0 vertex can be formulated as,

$$\begin{aligned} \Gamma_{t\bar{c}h} &= i\,\overline{u}_c(k_2)\,(F_L P_L + F_R P_R)\,u_t(k_1)\,, \\ F_{L,R} &= F_{L,R}^V + F_{L,R}^S\,, \end{aligned} \tag{22}$$

which contains the vertex corrections (from scharm–scharm–gluino, scharm–stop–gluino and stop–stop–gluino triangle loops), and the self-energy corrections (from scharm-gluino and stop–gluino loops). The one-loop vertex corrections in our Type-A1 scheme are

$$\begin{aligned} F_L^V &= \frac{\alpha_s}{3\pi}\sum_{j,k}\lambda_{jk}^L m_t (C_0 + C_{11})(m_h^2, m_t^2, 0; m_{\tilde{u}_j}, m_{\tilde{g}}, m_{\tilde{u}_k}), \\ F_R^V &= \frac{\alpha_s}{3\pi}\sum_{j,k}\lambda_{jk}^R m_{\tilde{g}} C_0 (m_h^2, m_t^2, 0; m_{\tilde{u}_j}, m_{\tilde{g}}, m_{\tilde{u}_k}), \end{aligned} \tag{23}$$

where $\tilde{u}_k \in (\tilde{c}_2, \tilde{t}_1, \tilde{t}_2)$, and (C_0, C_{11}) are the 3-point Passarino-Veltman C-function. $\lambda_{jk}^{L,R}$ is the product of relevant $h - \tilde{u}_j - \tilde{u}_k$ and $\tilde{u}_k - \tilde{g} - t(c)$ couplings, derived with the squark-rotation (9). The Type-A1 self-energy corrections are,

$$\begin{aligned} F_L^S &= 0\,, \\ F_R^S &= \widetilde{F}_0 \frac{\alpha_s s_\theta}{3\pi}\frac{m_{\tilde{g}}}{m_t}\left[B_0(0; m_{\tilde{g}}, m_{\tilde{t}_2}) - B_0(0; m_{\tilde{g}}, m_{\tilde{t}_1})\right], \end{aligned} \tag{24}$$

with B_0 the 2-point Passarino-Veltman function and s_θ given in (9) for $y = 0$. $\tilde{F}_0$ denotes the tree-level $h^0 - t - \bar{t}$ coupling, and is given by $\widetilde{F}^0 = (m_t/v)(\cos\alpha/\sin\beta)$. Again, in Eq.(23)-(24), we ignore the tiny sub-leading terms suppressed by powers of $m_c/m_{t,\tilde{g}}$. The form factors $F_{L,R}^{V,S}$ in Type-A2 can be obtained from (23)-(24) via exchanges of $L \leftrightarrow R$ and $x \to y$ everywhere.

4. Radiative Higgs Signatures at Colliders

For $cbH^\pm$ couplings, our analysis shows $F_{L,R}$ to be sizable, typically around $0.03 - 0.18$ for $(x,\, y) \simeq 0.5 - 0.9$, $(A, \widetilde{m}_0) \simeq 0.5 - 2\,\text{TeV}$, and $\tan\beta \simeq 15 - 50$. The K-factor, defined as $K = \left(F_L^2 + F_R^2\right) / \left(F_L^{0^2} + F_R^{0^2}\right)$, typically ranges in $\sim 2 - 5$. Fig. **??**(a) gives the sample production cross sections of $H^\pm$ via $p\bar{p}/pp \to H^\pm X$ at the Tevatron and LHC, where we set $(\mu, m_{\tilde{g}}, \widetilde{m}_0) = (300,\, 300,\, 600)\,\text{GeV}$, $(A, -A_b) = 1.5\,\text{TeV}$, $\tan\beta = (15,\, 50)$, and $x = 0.75$ for Type-A1. The rates for other values of x can be obtained by rescaling the K-factors [cf. Fig. **??**(b)-(c)]. The s-channel partonic fusion processes $cb \to H^\pm$ (with the SUSY loop corrections) and $cs \to H^\pm$ are both computed, including the next-to-leading order (NLO) SM-QCD corrections [12]. In Fig. **??**(a), the cross sections from the SUSY contributions $F_{L,R}^{S,V}$ dominate over that from the CKM-suppressed $F_{L,R}^0$ significantly. For $m_H \gtrsim 190\,\text{GeV}$, $H^\pm$ mostly decay into tb, and for $m_H \lesssim 190\,\text{GeV}$, $\tau\nu$ channel dominates. When $H^\pm$ mass is above the threshold of $W^\pm h^0$, the $W^\pm h^0$ channel (with $W \to \ell\nu$ and $h^0 \to b\bar{b}$) can be important as well [12]. The SM production of tb (WZ and Wh^0) at the Tevatron Run-2 has been well studied [11]. Thus, analyzing the invariant mass distribution of tb (Wh^0) is important for further discriminating our s-channel resonance signals from the pure SM backgrounds [12]. The solid curves of Fig. **??**(a) show that the Tevatron can access $H^\pm$ signals for m_H up to $\sim 300\,\text{GeV}$ with a planned luminosity of 2–20 fb^{-1} per detector, while the LHC can probe full

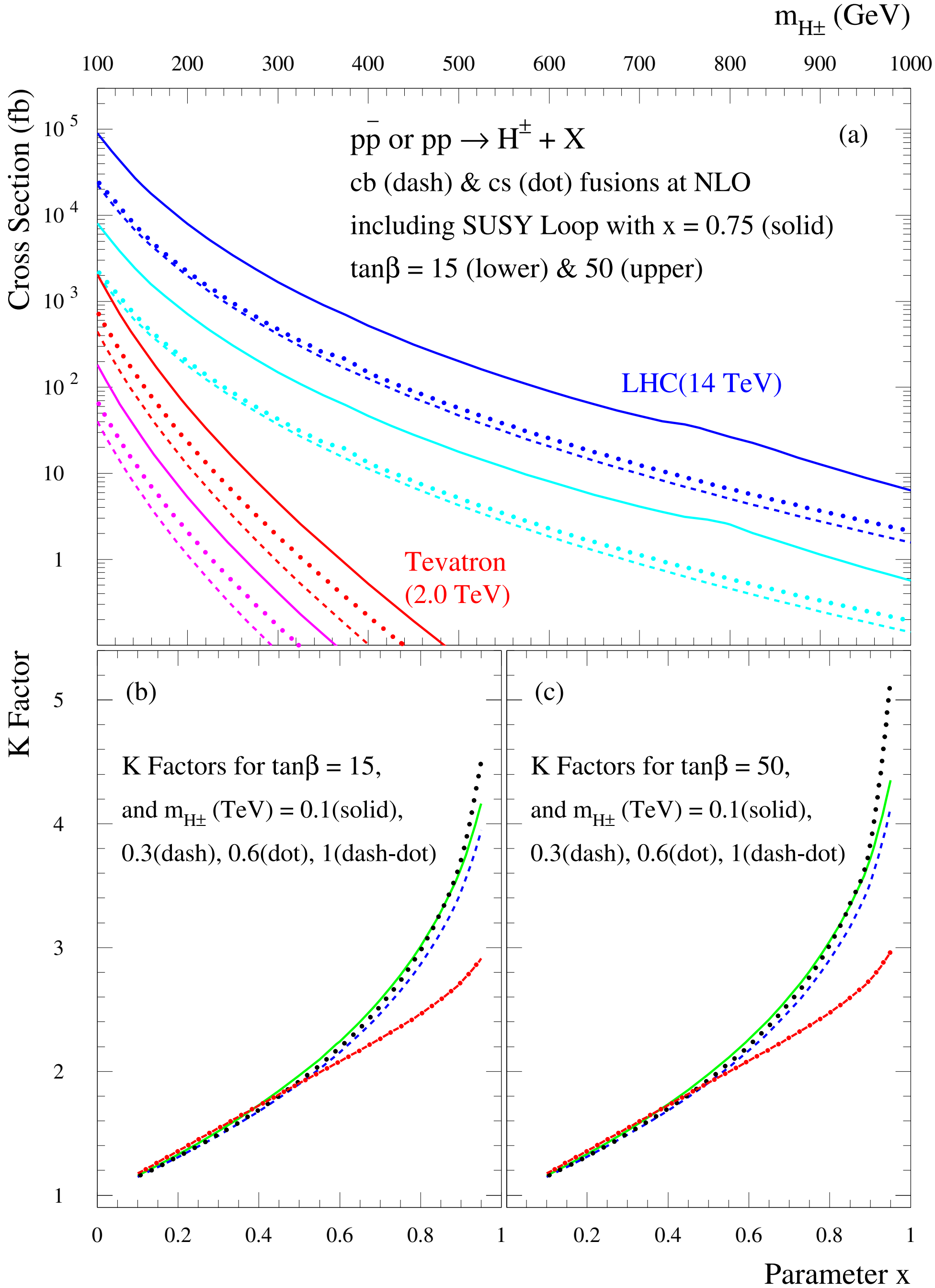

Figure 1: (a): $H^{\pm}$ production cross sections via cb (and cs) fusions at hadron colliders are shown as lower (upper) set of curves for sample inputs $\tan\beta = 15\ (50)$ and $x = 0.75$. (b) and (c): The factor $K = \left(F_L^2 + F_R^2\right) / \left(F_L^{0\,2} + F_R^{0\,2}\right)$ for $H^{\pm}bc$ vertex is depicted as a function of parameter x and for $\tan\beta = (15,\,50)$.

mass-range of $H^{\pm}$ with a luminosity of 100–200 fb^{-1}. These encouraging results strongly motivate more elaborated detector-level Monte Carlo simulations to quantify the discovery potentials at the Tevatron and LHC.

Table III Br[$t \to c\, h^0$] $\times 10^3$ is shown for a sample set of Type-A1 inputs with $(\widetilde{m}_0, \mu, A) = (0.6, 0.3, 1.5)$ TeV and Higgs mass $M_{A^0} = 0.6$ TeV. The three numbers in each entry correspond to $x = (0.5,\ 0.75,\ 0.9)$, respectively.

$m_{\tilde{g}}$	$\tan\beta = 5$	20	50
100 GeV	(.011, .10, .81)	(.015, .19, 4.6)	(.016, .21, 7.0)
500 GeV	(.011, .09, .41)	(.015, .13, 1.0)	(.016, .14, 1.2)

For $t \to ch^0$, the decay width is given by,

$$\Gamma(t \to ch) = \frac{m_t}{16\pi}\left[1 - \frac{m_h^2}{m_t^2}\right]^{\frac{1}{2}} \left(F_L^2 + F_R^2\right) . \tag{25}$$

Thus, the braching ratio is deduced as, $\mathrm{Br}[t \to ch^0] \simeq \Gamma[t \to ch^0]/\Gamma[t \to bW]$, to good accuracy. We will not consider possible SUSY decay channels of the top quark with R-parity nonconservation.

In the minimal SUSY-FCNC scheme-A and -B, the numerical analysis shows the braching ratio $\mathrm{Br}[t \to ch^0]$ can be typically as large as $10^{-3} - 10^{-5}$ (cf., Table III for Type-A1) over sizable parameter space where the lightest h^0 has a mass around 110–130 GeV. Very similar results to Table III are also obtained for Type-A2 and -B2 models. The LHC with an integrated luminosity of 100 fb^{-1} will produce about 10^8 t and $\bar{t}$ events [15] and thus has great sensitivity to discover this decay channel. Some recent model-independent Monte Carlo analyses [16] showed that the LHC (100 fb^{-1}) is able to measure $\mathrm{Br}[t \to ch^0]$ down to the level of 4.5×10^{-5} at 95% C.L. The future Linear Colliders will also have good sensitivity to observe this decay channel with the high luminosity and much clean background.

In summary, motivated by the existing theoretical and experimental bounds, we have constructed the minimal FCNC schemes for the squark mass-terms and scalar trilinear interactions and find large $O(1)$ mixings among top- and charm-squarks fully feasible. We support this feature by further providing a class of new models with horizontal $U(1)$ symmetry which also explains the quark-mass/mixing hierarchies and the natural SUSY μ-parameter. As applications, the dominant SUSY radiative corrections to the $b - c - H^{\pm}$ and $t - c - h^0$ couplings are analyzed in our minimal schemes without mass-insertion approximation. These radiative couplings can be significant to induce new discovery signatures of the supersymmetric Higgs bosons at the Tevatron Run-2 and the LHC.

Acknowledgments

I thank C.-P. Yuan and J. L. Diaz-Cruz for productive collaborations, and G. L. Kane, D. A. Dicus and Y. Nir for valuable discussions. This work was supported by U.S. DOE under Grant DE-FG03-93ER40757.

References

[1] See, for instance, reviews in "Perspectives on Supersymmetry", ed. G. L. Kane, World Scientific Publishing Co., 1998.
[2] S. Khalil, J. Phys. G**27**, 1183 (2001), [hep-ph/0011330], and references therein.
[3] A. Masiero and H. Murayama, Phys. Rev. Lett. **83**, 907 (1999), [hep-ph/9903363].
[4] J.L. Diaz-Cruz, H.-J. He, C.-P. Yuan, hep-ph/0103178, Phys. Lett. B (to appear), and work in preparation.
[5] For a nice review, M. Misiak, S. Pokorski, J. Rosiek, "Supersymmetry and FCNC Effects", hep-ph/9703442, in *Heavy Flavor II,* pp. 795, eds., A. J. Buras and M. Lindner, Advanced Series on Directions in High Energy Physics, World Scientific Publishing Co., 1998, and references therein.

[6] J. A. Casas and S. Dimopolous, Phys. Lett. B**387**, 107 (1996), [hep-ph/9606237].
[7] H.-J. He and C.-P. Yuan, Phys. Rev. Lett. **83**, 28 (1999), [hep-ph/9810367].
[8] E.g., Y. Nir and N. Seiberg, Phys. Lett. B**309**, 337 (1993), [hep-ph/9304307].
[9] C. D. Frogatt and H. B. Nielsen, Nucl. Phys. B**147**, 277 (1979).
[10] Y. Nir, M. Leurer, and N. Seiberg, Nucl. Phys. B **309**, 337 (1993) [hep-ph/9212278]; Nucl. Phys. B **420**, 468 (1994) [hep-ph/9310320].
[11] A. Meidei and R. Brock, Fermilab TeV2000 Report, 1995.
[12] C. Balazs, H.-J. He, C.-P. Yuan, Phys. Rev. D**60**, 114001 (1999), [hep-ph/9812263].
[13] E.g., B. Mele, S. Petrarca, and A. Soddu Phys. Lett. **B**435, 401 (1998), [hep-ph/9805498]. G. Eilam, J. L. Hewett, and A. Soni, Phys. Rev. D**44**, 1473 (1991) and Erratum, D**59**, 039901 (1999).
[14] For a recent review, see, *e.g.*, J. Solà, talk presented at the 5th International Symposium on Radiative Corrections, Carmel, CA, USA, Sept. 11-15, 2000 [hep-ph/010294], and references therein.
[15] For a recent review, see, *e.g.,* M. Beneke, *et al.*, “Top Quark Physics”, in the Report of the 1999 CERN Workshop on SM physics (and more) at the LHC, [hep-ph/0003033].
[16] J. A. Aguilar-Saavedra and G. C. Branco, Phys. Lett. B**495**, 347 (2000), [hep-ph/0004190].